J Stat Phys (2008) 133: 1083–1105
DOI 10.1007/s10955-008-9652-6

Stochastic Description of Traffic Flow

Timur Alperovich · Alexandros Sopasakis

Received: 13 June 2008 / Accepted: 14 November 2008 / Published online: 22 November 2008
© Springer Science+Business Media, LLC 2008

Abstract We propose a traffic model based on microscopic stochastic dynamics. We built a Markov chain equipped with an Arrhenius interaction law. The resulting stochastic process is comprised of both spin-flip and spin-exchange dynamics which models vehicles exiting, entering and interacting in a two-dimensional lattice environment corresponding to a multi-lane highway. The process is further equipped with a novel look-ahead type, anisotropic interaction potential which allows drivers/vehicles to ascertain local fluctuations and advance to new cells forward or sideways. The resulting vehicular traffic model is simulated via kinetic Monte Carlo and examined under both, typical and extreme traffic flow scenarios. The model is shown to correctly predict both qualitative as well as quantitative traffic observables for any highway geometry. Furthermore it also captures interesting multi-scale phenomena in traffic flows after a simulated accident which lead to oscillatory, dissipating, traffic waves with different periods per lane.

Keywords Multi-lane traffic flow · Anisotropic look-ahead rule · Markov Chain · Spin-flip/spin-exchange dynamics · Arrhenius potential · Kinetic Monte Carlo

1 Introduction

One way of perceiving vehicle dynamics, is as an ever changing dynamical system whose behavior can be easily described only for the special cases of either very low or very high (jam) vehicle concentrations. A description of traffic interactions and vehicle behavior is elusive however for a large range of concentrations which in fact happens to be the most interesting since modern highways seem to mostly operate within that range. Roughly speaking that range lies between 0.2 and 0.8 (normalized) vehicle concentrations. A number of

T. Alperovich
Univ. of Massachusetts at Amherst, 710 North Pleasant Street, Amherst, MA 01003, USA

A. Sopasakis (✉)
Dept. of Math. & Stat., Univ. of North Carolina at Charlotte, 2101 University City Blvd., Charlotte, NC 28223, USA
e-mail: asopasak@uncc.edu

nonlinear phenomena have been observed for vehicles within this range of vehicle concentrations. Some of these include shock waves, phase transitions [19, 30], and are responsible for the ensuing traffic break-down [22, 27] which become apparent as nonlinear dynamics [35, 42, 49] overtake the system. Identification of these phenomena is clearly a difficult task which we will to undertake in this work by first trying to establish their interactions at the microscopic level.

Traffic congestion accounts, to name just a few, for significant impact to the environmental, direct and indirect pressure to economic markets as well as the resulting and unavoidable diminishing size of our resources all of which play a major part in what we term "modern" problems for the 21st century. As a relevant example consider that between 1990 and 2004 motor vehicle traffic in Great Britain increased by 21%. Similarly during that same period CO_2 emissions also increased by 10% even though significant technological improvements have allowed decoupling of emissions to pollution from nitrogen oxides (NOx) and particulate (PM10). It is notable that even though technology improved the energy consumption for transport increased by 15% during this same period. This trend will reach its unavoidable saturation limit sooner rather than later. A solution is not only necessary but also inevitable due to the seriousness of the repercussions of not having one.

There are a number of approaches and respective types of models striving to describe traffic behavior. Models can be divided into the following categories [1, 9]: analytical (using actual data and theoretical considerations), descriptive (applying theoretical principles), deterministic (without random effects) and empirical (using statistical analysis of actual data). Models often tend to belong to more than one of these categories however and stochastic techniques as well as computer simulations are commonly employed.

It seems daunting however for any *deterministic type* model [37, 40] of vehicular traffic to capture these multivalued and transitional effects observed for concentrations above c_{crit} (approximately 20% of jam density). This is probably the reason that a number of such models have been criticized [5, 33, 36, 38, 39] thus leading to subsequent improvements more recently [3, 14, 42]. Due to their nature deterministic models lack the descriptive capabilities, especially in terms of capturing transient behavior, which are possible through a stochastic model, and which we hope to entertain here.

In contrast cellular automaton (CA) models, due to their microscopic structure, are able to re-produce a much richer behavior for traffic flow [15, 31, 41]. CA models are discretized in space, time and velocity and mimic car movement through elementary updating mechanisms which model acceleration and slowing down effects due to interactions with other cars. To further enhance interactions and complex behavior however more advanced CA models include a random *ad hoc* slowing down term thus leading to more realistic and interesting traffic behavior. In some cases the results of the simulation work as a feed-back mechanism in order to discover the best placement as well as type of noise term to be used. A variety of approaches [17, 20, 31, 32, 40] have therefore been proposed and subsequently applied to these simple updating mechanisms. It is necessary to emphasize that in this work we do not propose a CA type model. Along these lines the approach which is followed here will be shown to have distinct differences and/or benefits over CA type models. See Sect. 5 for further details.

We present a fully stochastic traffic model based on a carefully constructed Markov process. This stochastic process moves vehicles and keeps track of their interactions in the highway while keeping physical limitations in check. While building this process we take into account physical limitations about geometry, vehicle speed limits, vehicle sizes, etc. Multi-lane highways necessitate use of anisotropy type stochastic potentials as a lane changing mechanism. On the other hand, inclusion of entrances and exits require non-conservative

type stochastic dynamics thus changing drastically the overall system behavior. Although the model derived here is mathematically rigorous it also becomes, as we will show with our Monte Carlo simulations, a useful real-time, predictive tool for traffic evolution, development and future roadway design. In that respect the actual applications of such a model could be extensive.

We outline below the work which is presented here. We start by building the Markov chain in Sect. 3. The details about potential interactions are presented in Sect. 3.1 and the corresponding dynamics are given in Sect. 3.3.

The effects of passing and lane changing are relatively minor in free flow conditions. Clearly this is not the case in congested traffic where lane changing type interactions can be responsible for unstable traffic conditions and may result in chaotic behavior both in theory and in practice. The multi-lane stochastic traffic flow model is developed in Sect. 3.4 and is shown to capture some of the essential features which, based on observations, are expected to exist in any traffic stream.

Once our stochastic model and its dynamics have been fully presented we outline similarities and main differences or benefits when compared against other well-known traffic flow modeling approaches in Sect. 5 Furthermore, in Sect. 5.1 we also summarize the macroscopic derivations carried out in [44]. This is a very important feature which our model possesses and further distinguishes it from other microscopic models.

The full stochastic model developed here can be easily implemented numerically via use of kinetic Monte Carlo simulations. The resulting algorithm can handle heavy traffic and produces predictions in real time. We test the resulting model under a variety of common traffic conditions and observe or compare the developing flow against actual data when possible in Sect. 4. Our findings are summarized in the conclusions, Sect. 6.

There are several different data collection methods depending on the space and time scales of observables we are interested in monitoring. On the other hand there are large variations directly related to the collection method used for seemingly similar traffic data. Therefore in order to properly compare our model against actual traffic data we must take into account the data collection method employed. Furthermore the numerical validation of the model via simulations must sample data in the same manner as actual data is collected in the field so that reliable comparisons may be possible. The developing theory therefore must depend and account for measurement capability [6]. The link between actual data collection and simulated traffic sampling is therefore important and is examined in the Appendix.

2 Known Traffic Phases and Transition Regimes Based on Observation

Although simplistic, the following rough break-down of main traffic states, under different traffic conditions, gives a good overview of knowledge in the field. The guide presented below also provides a chart of expectations for any reasonable traffic model.

One way to quantitatively categorize traffic states is the Level Of Service (LOS) [51]. Just recently the Transportation Research Board, the government entity responsible for all transportation in the United States, published an update to the Highway Capacity Manual (HCM) [8] which based on observations defines the range of LOS from A to F according to density measured in pc/mi/ln (passenger cars per mile per lane). The HCM categorizes traffic states from stable, in which case vehicles can drive at their desired speeds, to unstable, where small fluctuations in vehicle speeds can trigger large deviations in those speeds and the occurrence of stop-and-go traffic waves. Unstable traffic states are responsible for a reduction in highway capacity. Highway *capacity*, for a given section of roadway, is defined

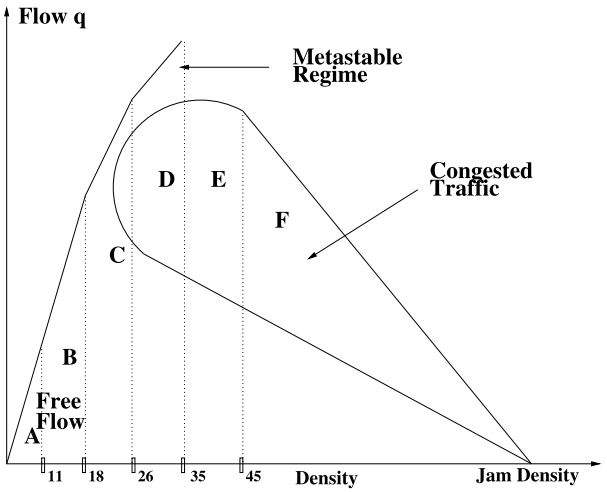

Fig. 1 The fundamental diagram (flow-density relationship) depicting some of the major traffic states. The numbers in the x-axis represent vehicles per mile and are known approximately based on the observational record

to be the *maximum* number of vehicles which can pass a given point in one hour under the best roadway traffic conditions.

In summary, according to the HCM, the behavior of traffic and its stability based on density measured in pc/mi/ln according to [8] is given as follows:

A (0–11): Free-flow. Vehicles obtain their desired driving speeds. Low densities and high speeds are prevailing. This is a stable traffic state.
B (11–18): Most vehicles are able to maintain their desired speeds without having to change lanes. Also a stable traffic state.
C (18–26): Desired vehicle speeds start getting restricted. Drivers are not readily able to change lanes. This is also a stable traffic state.
D (26–35): Restrictions in maneuvering influence the desired speeds which start to decrease. These conditions can be tolerated only for short time periods otherwise traffic stability is at risk. This traffic state therefore is on the verge of instability.
E (35–45): Appearance of stop-and-go traffic waves and queues. Traffic is operating near the maximum highway capacity. Unstable traffic conditions.
F (>45): Low vehicle speeds and low flows are prevailing. Highway is operating below capacity and traffic jams with complete stops appear. This is also an unstable traffic state.

Most everyone is familiar with free flow and congested traffic and Fig. 1 depicts these in a simple diagram. Congested traffic however can substantiate in several different forms and may include the so called "wide moving jams" or "synchronized" traffic phenomena. A wide moving jam, is a localized structure, such as a traffic wave, with width which is larger than its front and propagates unchanged against the direction of traffic [19, 40]. Synchronized traffic, on the other hand, is characterized by high vehicle flows which surprisingly can sustain also increasing vehicle velocities [19, 40]. Naturally this is a recipe for disaster since sooner or later the traffic must break down with a number of other interesting traffic states yet to be discovered. A metastable region, as also marked on our diagram in Fig. 1, is a result of some type of synchronized traffic phenomenon where drivers try to attain their desired speed even though vehicle densities are increasing. Once again the observed capacity drop and ensuing, seemingly chaotic, behavior is inevitable.

Here we attempt a new approach in traffic modeling which results in a fully stochastic model for multi-lane vehicular traffic with entrances and exits. The model which we propose

is based on the principles first introduced in [43] for single lane traffic. The idea in [43] originates from developments in non-equilibrium statistical mechanics [16, 25, 46] and in particular more recent developments in microscopic Ising type systems [18]. The main idea however lies in [43] where the first fully stochastic traffic model is introduced in the one-lane highway setting.

In this work we construct a multi-lane model and equip it with a combination of different stochastic dynamics which allow us to explore any size of two-dimensional geometries as well as entrances and exits of interacting vehicles. Furthermore we combine a novel, energy driven, stochastic noise process in conjunction with an anisotropic type interaction potential in an attempt to describe the different phases of traffic and the vehicular behavior which may arise at any concentration. Vehicles advance based on the energy profile of their surrounding traffic through a look-ahead one-directional interaction potential. The model displays important similarities when compared to observed behavior from actual traffic data and, as we will show, is able to predict a number of vehicular traffic characteristics.

A major advantage which further differentiates this model is that it relies on a small number of free parameters which are directly linked to easily observed physical traffic characteristics (see Sect. 4.1). Therefore due to its inherent simplicity this model can also be analyzed mathematically.

3 Model Overview and Energy Description

In this section we present the basic stochastic spin-exchange type dynamics which dominate vehicle interactions while interacting with other vehicles within the highway as well as more generally the environment through spatial and temporal events. We start by providing the relevant notation. We consider, for now, a loop highway. We let $\mathcal{L}_n = \{1, 2, \ldots, n\}$ and $\mathcal{L}_m = \{1, 2, \ldots, m\}$ and define our physical space as a two-dimensional, periodic lattice $\mathcal{L} = \mathcal{L}_n \times \mathcal{L}_m$, which is partitioned into $n \cdot m = N$ cells. Here n denotes the number of lanes and m denotes the horizontal number of cells. Therefore, each lattice cell location $x \in \mathcal{L}$ is defined by its horizontal cell number x_k for $1 \leq k \leq m$ and its lane number, x_l for $1 \leq l \leq n$, as follows

$$x = (\text{horizontal cell number}, \text{lane number}) = (x_k, x_l). \tag{1}$$

The identification from particle dynamics to vehicles is understood in the simplest possible setting: on each of the lattice locations $x \in \mathcal{L}$ we define an order parameter $\sigma(x)$ via,

$$\sigma(x) = \begin{cases} 1, & \text{if a vehicle occupies site } x, \\ 0, & \text{if site at } x \text{ is empty (no vehicle).} \end{cases} \tag{2}$$

A spin configuration σ is an element of the configuration space $\Sigma = \{0, 1\}^{\mathcal{L}}$ and we write $\sigma = \{\sigma(x) : x \in \mathcal{L}\}$ denoted by $\sigma(x)$ the spin at x.

We extend the usual Ising type particle interactions to vehicles and derive a corresponding microscopic stochastic model. This procedure should be successful assuming we can correctly capture and describe mathematically, how vehicles interact.

We start by obtaining suitable interpretations of many of the usual parameters of Ising systems and in many instances absorb as many of those parameters as possible in order to simplify our model and adapt it better to vehicular traffic.

Since there are $|\mathcal{L}| = mn$ sites on the lattice then the system can be in any of $2^{|\mathcal{L}|}$ possible states. The local situation at each of those states is appraised by the interaction potential J.

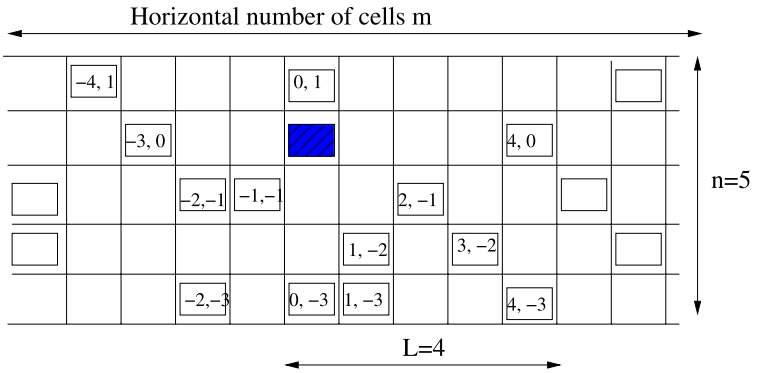

Fig. 2 The values for each car in a highway as referenced by the marked car. We use the format $(y_k - x_k, y_l - x_l) =$ (difference in lane number, difference in horizontal cell number) where $1 \leq k \leq m$ and $1 \leq l \leq n$. In this example we have assumed a $n = 5$ lane highway with a look-ahead of $L = 4$ cells. Note that based on the potential function J, in (3), all negative differences in lane number automatically produce a 0 contribution and therefore no moves backwards

We let J denote an asymmetric short range inter-vehicle interaction potential,

$$J(y, x) = V\left((y - x)_d / L\right), \quad x, y \in \mathcal{L} \tag{3}$$

where L denotes the potential radius and $y - x = (y_k, y_l) - (x_k, x_l)$. This distance between vectors x and y is defined through,

$$(y - x)_d := y_k - x_k \tag{4}$$

where $1 \leq l \leq n$ and $1 \leq k \leq m$. Note that the distance between locations x and y in (3) may have a positive or negative sign. In the case that the sign is negative we assign a value of the potential equal to 0 through (5) which immediately implies that vehicles cannot perform moves backwards. In the opposite case that the difference between x and y is positive then there is a contribution from that potential. We therefore let $V : R \to R$ and set,

$$V(r) = 0, \quad r \in R^- \quad \text{and} \quad V(r) = 0 \quad \text{for } r \geq 1.$$

A relevant clarifying schematic can be found in Fig. 2. In the simulations we choose a simple, uniform, potential of the form,

$$V(r) = \begin{cases} J_0 & \text{if } 0 \leq r < 1, \\ 0 & \text{otherwise} \end{cases} \tag{5}$$

where J_0 is a parameter which based on its sign describes attractive, repulsive or no-interactions (note that we can easily adapt a non-constant value of J_0 which would be more realistic, such as a Maxwellian, or otherwise). Since vehicles naturally try to move toward the empty space in the highway we must enforce repulsive interactions. We therefore implement, piecewise constant, $J_0 = 1$, short range local interactions. At the same time (5) indirectly enforces simple but necessary rules for vehicles, such as no negative speeds (since V is zero for moves backward). Similarly, since we set $0 < r < 1$ (i.e. short range interactions), it is easily seen that vehicles only react to local, and based on the above derivation, forward,

traffic conditions and stimuli, as would be expected in real traffic situations. In the simulations which will follow we let $L = 4$. This potential radius in effect corresponds to vehicles (or drivers) being able to look-ahead for up to 4 cells in order to evaluate the status of traffic in front of them and make a more sensible decision as to which cell to move to next based on the potential strength, (3). See Sect. 4.1 for more details on the physical interpretation of this parameter in relation to cell site.

3.1 Interaction Potential

In this model we implement spin-exchange Arrhenius dynamics in order to simulate vehicle movement and their interactions while in the highway. We refer to [23] and ideas in [43] for other possibilities. Under this, Arrhenius type, engine the simulation is driven based on the *energy barrier* a particle has to overcome in changing from one state to another. During such a spin-exchange between nearest neighbor sites x and y the system will actually allow the order parameter $\sigma(x)$ at location x to exchange sign with the one at y. This is interpreted as advancing a vehicle forward from x to y. The rate at which a process will do this for spin-exchange Arrhenius dynamics is defined [23] as,

$$c(x, y, \sigma) = \begin{cases} c_0 \exp[-U(x)], & \text{if } \sigma(x) = 1,\ \sigma(y) = 0, \\ 0, & \text{otherwise} \end{cases} \tag{6}$$

where

$$c_0 = 1/\tau_0 \tag{7}$$

with τ_0 the characteristic or relaxation time for the process. For one-lane highway $y = y_k = x_k + 1$. For an n-lane highway however y is such that

$$\begin{aligned} y_l &= x_l + 1 \quad \text{for moves to the left,} \\ y_l &= x_l - 1 \quad \text{for moves to the right,} \\ y_k &= x_k + 1 \quad \text{for moves forward.} \end{aligned}$$

As will become clear in the simulations, in Sect. 4, the two free parameters c_0 (or τ_0) and J_0 are directly related to known traffic observables and will therefore be easy to calibrate (see Sect. 4.1). In (6) $U(x)$ denotes the inter-vehicle interaction potential which is comprised of contributions from exchange interactions U_e, anisotropy interactions U_α as well as an external potential $h(x, t)$,

$$U(x) = U_e(x) + U_\alpha(x, x_*) + h(x, t) \tag{8}$$

all of which will be defined in detail in the next section. We note however that the external potential $h(x, t)$ in the potential above is allowed to vary in both space and time if so desired. In that case h can therefore account for temporal and spatial traffic situations which in effect may simulate phenomena such as rush hour traffic, local weather anomalies etc.

What really differentiates one move from other possible moves forward is (8). That equation "detects" other vehicles forward and adds penalty terms to the overall potential thus making moves in crowded situations less likely. In the opposite case however where there are less vehicles forward moves will be more likely to occur since the overall potential will have reduced penalty terms. For now, to make things simple, we allow only uniform potentials and therefore the penalty term contribution for vehicles ahead, regardless of distance, is equivalent.

The stochastic process $\{\sigma_t\}_{t\geq 0}$ constructed above is a continuous time, jump, Markov process on $L^\infty(\Sigma; R)$ with generator [23],

$$(Mf)(\sigma) := \sum_{x\in\mathcal{L}} c(x, y, \sigma)[f(\sigma^x(y)) - f(\sigma(y))], \quad \text{for all } 0 < y \in \mathcal{L} \tag{9}$$

for any bounded test function $f \in L^\infty(\Sigma; R)$ with $c(x, y, \sigma)$ defined in (6). Here $\sigma^x(y)$ denotes the configuration after a change in the value of the cell at x such that, $\sigma^x(y) = 1 - \sigma(x)$ if $y = x$ and $\sigma^x(y) = \sigma(y)$ otherwise. Therefore observables f (test functions) evolve with the rule [23]

$$\frac{d}{dt}\mathbf{E} f(\sigma_t) = \mathbf{E}(Mf)(\sigma) \tag{10}$$

which is equivalent to Dynkin's formula. In the sections which follow we give all the details regarding the type of interactions used in the potential U comprising (8).

3.2 Spin-Exchange Dynamics

The proper dynamics for vehicles interacting on the highway, which also allow for mass conservation, are exchange dynamics. In that respect we model how vehicles, which are denoted by $\sigma = 1$, interact and exchange values with empty cells around them, denoted with $\sigma = 0$, thus signifying a move. We start by first defining this type of short range interactions [13] via,

$$U_e(x) = \sum_{z\neq x} J(x, z)\sigma(z) \tag{11}$$

with J as in (3). Note that the exchange, due to the specific construction of the interaction potential J in (3), can take effect if and only if the location at x is occupied while the location at y is not. In that respect vehicles are restricted from colliding or willingly performing such an unrealistic move for vehicular traffic. On the other hand we should point out that the model does allow for modeling vehicle collisions as well. In that respect we refer to Sect. 4.3.1 of the manuscript where such a scenario is entertained. Similarly note that due to the construction of the interaction potential V in (5) it is not possible for an exchange move backward to occur since the probability for such an event would be 0. Thus exchange interactions, as modeled here, only allow moves ahead as well as sideways to occur. More details about how moves sideways are performed will be provided in Sect. 3.4 later.

3.3 Spin-Flip Dynamics and Entrances/Exits

In this model we implement both spin-flip and spin-exchange Arrhenius dynamics. The spin-flip mechanism models vehicles interacting while entering or exiting the highway. Thus the overall vehicle density on the highway is changing. During a spin-flip the system will actually allow the order parameter $\sigma(x)$ at location x to change sign. Note however that this move does not reciprocate by exchanging the spins at each location as the spin-exchange mechanism (6) does. This new spin-flip mechanism is interpreted instead as placing (removing) a vehicle at (from) x if $\sigma(x) = 0$ (1). The rate at which a process will do this for spin-flip Arrhenius dynamics is [47],

$$c^{sf}(x, \sigma) = \begin{cases} c_0^{sf} e^{-\beta U_{sf}(x)}, & \text{when } \sigma(x) = 0, \\ c_0^{sf} & \text{when } \sigma(x) = 1, \end{cases} \tag{12}$$

where,

$$U_{sf}(x) = \sum_{z \neq x} J(x, z)\sigma(z) \tag{13}$$

and

$$c_0^{sf} = 1/\tau_{sf}.$$

Here τ_{sf} denotes the characteristic or relaxation time for the spin-flip process. Therefore the probability of spin-flip at x during time $[t, t + \Delta t]$ is, $c^{sf}(x, \sigma)\Delta t + O(\Delta t^2)$.

Note that with the mechanism introduced in (12) we can now account for vehicles entering or exiting the highway at specific locations x. We have therefore marked a series of such locations on the lattice as entrances or exits. Each such entrance or exit consists of approximately 5 or 6 cells which translates to a total distance of approximately 120 feet as can be seen in Fig. 5. When vehicles in the highway approach an entrance then other vehicles may appear on the lane close to that entrance. Similarly when vehicles approach an exit and they are positioned in the lane near the exit they have the choice of leaving the highway using this spin-flip mechanism. More details of how this is implemented numerically can be found in the simulations Sect. 4 as well as in the pseudo-code provided in Appendix 1.

Considering a multi-lane highway requires different dynamics than those used in the one-lane case. Special attention to application of the proper vehicle interaction potentials is needed. Note that all vehicles in the same latitude of a multi-lane highway would have essentially equivalent potential $U(x)$ and therefore chances of advancing based on (6). In the section that follows we therefore introduce tools which differentiate among vehicles based on their lane positioning. We undertake this task next.

3.4 Anisotropic Interactions and Lane Changing

In Sect. 3 we established the main machinery which allows vehicles to either move forward in the highway based on local traffic conditions in front of them or exit/enter the highway based on exiting/entering ramp information. We now establish a specialized mechanism which will allow vehicles to also move laterally and in effect take advantage of empty space in a specific lane.

The novel mechanism which will be presented here for traffic flow can be easily adjusted to differentiate for driving rules according to the country/region it is applied. The lane changing dynamics which will be presented therefore can be used for either American, European or other standards of driving.

There are two possibilities for lane changing. Either the drivers must use only the left lane at all times or, for example, an American type system, where the driver may also use the right lane for passing. In the first case we have a so-called asymmetric lane changing rule while in the second case we have a symmetric type of potential. Both such rules can be easily adapted in our model via a simple modular mechanism. We follow ideas from [32] and [45] in terms of developing schemes which agree with observations of lane changing behavior.

Lane changing can be easily incorporated in our model by essentially adjusting the vehicle interaction potential U to contain an extra anisotropic term. This anisotropy will operate as a penalty term thus making it more taxing on the potential $U(x)$ to allow a move towards a lane which seems to be already congested. The interaction potential (8) is therefore designed to differentiate between two possible directional mechanisms: forward or sideways streaming (see Fig. 3). This overall lane changing mechanism will be added in (8) by augmenting

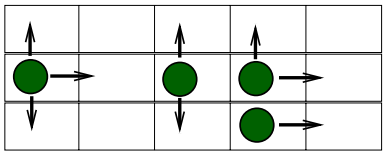

Fig. 3 Schematic of lane changing based on a 3 lane highway and local interactions

the interaction potential $U(x)$ with anisotropy interactions U_α, as follows,

$$U_\alpha(x, y) = \sum_{z_k = y_k}^{y_k + L} w\sigma(z) \tag{14}$$

where y denotes the location of the cell that the vehicle from x will move to. Once again we denote $y = (y_k, y_l)$ where y_k denotes the horizontal cell number and y_l the lane number. Here the value of the constant w is chosen based on preferences for moving forward or sideways. Note that if the car is moving to a new location y which has a number of empty cells in front of it then, according to the summation in (14) the penalty term will be small. Thus it will be more likely that the vehicle will actually move to that location y instead of another direction (see Fig. 3).

We let the parameter w vary based on direction as follows,

$$w = \begin{cases} w_l & \text{if } y = x_l + 1, \\ w_r & \text{if } y = x_l - 1, \\ w_f & \text{if } y = x_k + 1. \end{cases} \tag{15}$$

The notation $x_l + 1$ corresponds to a vehicle switching into the lane to its left while $x_l - 1$ denotes a move to the right lane. Finally $x_k + 1$ corresponds to a move forward without switching lanes. The values for the anisotropy constants w_l, w_r and w_f will be presented in the calibration Sect. 4.1. For realistic traffic conditions we always choose $w_f \gg w_l$ and $w_f \gg w_r$ which enforces the desire of motorists to move forward rather than switching lanes. Therefore, when cars have all possible choices of moving (left, right or forward), they would almost always elect to move forward.

Similarly we take $w_l > w_r$ which simulates the driver's preference to switch into the left rather than the right lane, ensuring the asymmetric lane-changing behavior which we wish to implement. Drivers will therefore remain in their lane until they meet a slow car, at which time they will most probably move into the new lane based on (14). This also results in the natural division of the highway into slow and fast lanes if an asymmetric potential is used. Note that we can easily modify (15) to implement symmetric lane-changing rules for American highways by setting $w_l = w_r$. In this way, a driver has equal probability of changing to either lane, given equivalent conditions in each lane.

Overall given (6) and (12) and the dynamics just described the combined probability of spin-flip at x or spin-exchange between x and y during time $[t, t + \Delta t]$ is,

$$c^{sf}(x, \sigma)\Delta t + c(x, y, \sigma)\Delta t + O(\Delta t^2). \tag{16}$$

In terms of traffic this is understood as the probability that a vehicle will enter/exit the highway at x or that a vehicle at location x will move to location at y. Note that if indeed there is already a vehicle at location y the corresponding probability will be zero, since we have designed a special asymmetric exclusion process, and therefore there will be no chance for this move to occur. In terms of further understanding rate (6) consider a free flow region

with just one vehicle at location x in the highway. In that case the potential $U(x) = 0$ for that vehicle and therefore $c(x, y, \sigma) = \exp(0) = 1$. Thus maximum probability of moving forward from x to y. In the opposite situation of a very crowded highway $U(x)$ would be large and positive thus reducing drastically the probability of advancing. In the case that the external field potential $h \equiv h(x, t)$ in (8) is also active (due to an accident, bad weather etc.) then $U(x)$ is penalized further impeding moving forward.

In our simulations, three possible spin exchanges were permitted (left, right and forward) and the way vehicles move can therefore be compared to the simulations in [32]. Nevertheless our simulations can be very easily adapted to allow other exchanges, such as diagonal moves although the value of this extra possibility may not be substantial. This can be understood as a vehicle advancing forward and switching lanes simultaneously.

In the multi-lane case, for the purposes of our simulations, we set our look-ahead parameter, L, to be four times the cell length. This allows drivers to appraise traffic up to four cells in front of them in all lanes in order to make an educated decision as to where to move to next. Four cells look-ahead corresponds to a physical viewing distance for each driver of approximately 88 feet forward on all lanes since each cell has size 22 feet.

4 Simulations and Kinetic Monte Carlo

One way to simulate this interacting system is by using two intertwined Monte Carlo algorithms. The algorithms are therefore responsible for moving vehicles according to their respective probabilities based on the description given in the microscopic Sect. 3. The main Monte Carlo algorithm keeps track of all vehicles in the highway while the second algorithm allows vehicles to enter or exit the highway.

Another method which can be used to simulate traffic behavior on a multi-lane highway with entrances and exits is to use a single Monte Carlo algorithm and the combined probability (16). This is in fact what we have used for all the simulations presented in this work. In this case therefore we compute simultaneously the rates of all vehicles either in the highway or those entering the highway.

We implement the Kinetic Monte Carlo (KMC) as follows: we start by calculating all the transition rates for each vehicle based on (6) for moves to nearest neighbor locations. Note that automatically based on our design (3) the moves to occupied locations always have rate 0. We calculate the total exchange rate for all vehicles (so as to create a measure) and we use a random number in order to choose one from among them. We perform the chosen move between locations x and y and update the simulation time by Δt which is equal to the inverse of the (already calculated) total rate for all vehicles. We repeat this process from the beginning until we have captured the dynamics of interest or simply have reached the end of time for our simulations (equilibration). Please see Appendix 1 where the details of the simulation are presented in a pseudo-code.

As expected a KMC algorithm produces no "null" steps [4] and therefore every iteration is a success. This is quite useful for the cases of high densities of vehicles or while reaching equilibration. Normally in such a situation a usual Monte Carlo algorithm would slow down performing moves less and less often staying idle simulation-wise for long periods of time. Our KMC algorithm however continues to choose and move vehicles at every single step by skipping the idle waiting and simply adjusting the simulation time by the appropriate amount, as if it had waited for that long. Note also that the simulation time is tracked in step 6 of the KMC pseudo-code provided above. During this time vehicles can enter, exit or move forward in the highway.

In all the examples considered we allow $L = 4$ in the calculation of the interaction potential, $U(x)$. Given the one-sided structure of this potential drivers are able to perceive traffic densities which are up to 4 vehicle lengths—plus safe distance—ahead of their vehicle. In the multi-lane examples, we multiply L by the number of lanes, so that drivers can look-ahead up to four vehicle lengths in *each* lane. However we have also run simulations (not presented here) with a look-ahead of 3 and 5 vehicle lengths and in the majority similar results were observed.

4.1 Calibration of Parameters

We define the length of each cell to be 22 feet. This allows for the average vehicle length plus safe distance. Therefore for a vehicle which has an average speed of 60 miles per hour we obtain a natural estimate of time to cross a cell, $\Delta t_{cell} = \frac{22 \text{ feet}}{60 \text{ miles/hour}} = \frac{1}{4}$ s. In most of the examples considered below we allow $L = 4$ nearest neighbors in the calculation of the interaction potential, $U(x)$. Given the structure of this potential (one-sided) this implies that drivers are able to perceive traffic densities which are up to 4 vehicle lengths (plus safe distance) ahead of their vehicle (or 4×22 feet $= 88$ feet look-ahead). In the multi-lane examples, we multiply L by the number of lanes, so that drivers can look-ahead up to four vehicle lengths in *each* lane.

The free flow velocity or desired velocity is decided in advance and set in the simulation through the free parameters J_0 and τ_0. We start by calibrating our code through these free parameters J_0, and τ_0 by first simulating a free flow regime (very few vehicles on the road) where we expect most vehicles to drive at their desired speed. For now we take the desired speed to be the same as the highway speed limit. Note however that the desired velocity could be easily adjusted to reflect other tendencies thus, indirectly, also taking into account cultural aspects in driving behavior.

We perform a trial simulation, such as the one presented in Fig. 4, in order to calibrate the desired velocity vehicles would like to drive at. Here we simulate a two-lane highway. As pointed out earlier the free parameter J_0 indirectly influences how drivers react to conditions in front of them and subsequently allows us to set the velocity of an upstream front (which for some highways is known to be approximately -15 ± 5 km/hour [12, 40]). We therefore pick τ_0 so that the desired vehicle speeds are approximately 60 miles/hour (see Fig. 4). Similarly we pick a value for J_0 so that the upstream shock velocity is approximately 11 m/h in agreement with [11, 50]. The resulting simulation for this calibration is shown in Fig. 4. Note that due to the stochasticity inherent in our simulation some vehicles will drive faster while some may drive slower than the average desired velocity chosen for this simulation. Also see Fig. 7 later where this variation in speeds is evident.

We can easily calibrate for the parameters τ_0 and J_0 in advance for any number of lanes as can be seen in Table 1. Note that these parameters once chosen do not need to be further adjusted and can be implemented in any traffic simulation which is described by these basic underlying characteristics. Note for example that parameters $\tau_0 = 1.7$ and $J_0 = 2$ would be used for an one-lane highway with an average desired velocity of 65 miles/hour. From the data in Fig. 4 we find that the traffic jams move backward in traffic with a speed of ≈ -10 miles/hour. We choose this value for the backward moving speed of the traffic jams in order to agree with the reported speed in [12, 40]. Overall, based on the results of simulations similar to Fig. 4, we can calibrate in advance the values of τ_0 and J_0 for a number of different desired speeds and lanes on any highway. Also note that other pairs of τ_0 and J_0 are possible which easily adjust the traffic model for different standards set in other countries or regions.

In the next few sections we choose the appropriate parameters from this table in order to give examples of traffic behavior under a variety of traffic lanes and desired speeds.

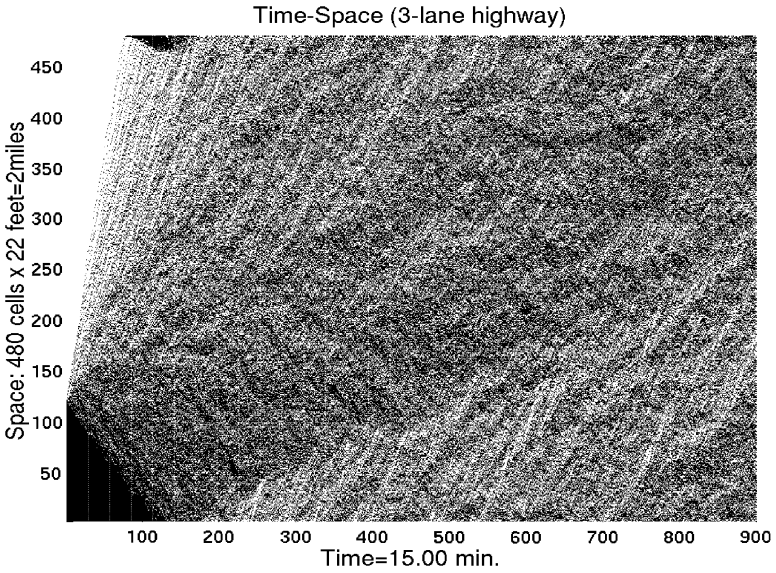

Fig. 4 Calibrating the free parameters τ_0 and J_0. In this example we simulate a multi-lane periodic highway which is 2 miles long. We choose τ_0 and J_0 so that the desired vehicle speeds are set at $\approx$60 miles/hour for free flow while the upstream shock velocity is set at ≈ -10 miles/hour in order to agree with observations [50]. This is a traffic release problem which illustrates behavior as a traffic light turns green at time $t = 0$ with 240 vehicles at rest. Vehicles occupying adjacent cells on this 3-lane highway are plotted in the same position x in the graph above

Table 1 A few examples of choices for parameters τ_0 and J_0 for highway traffic with the resulting desired vehicle velocities for free flow and upstream front velocities. The look-ahead parameter is chosen, based on physical considerations, to be $L = 4$, while the anisotropy constants for lane changing are chosen to be $w_l = 1$, $w_r = 1.5$ and $w_f = 4$

# of lanes	1	2	3	4
τ_0	1.7	2.0	1.9	1.9
J_0	2	0.6	0.4	0.3
Desired velocity (mph)	65	60	70	72
Upstream velocity (mph)	−9.9	−9.8	−10.4	−9.8

We also note that in our simulations we let entrances and exits to occupy more than a single cell on the highway. This once again produces a more realistic effect. We let entrances and exits occupy 5 adjacent cells, or a length of $5 \times 22 = 110$ feet, at a predetermined location on the highway. Naturally vehicles enter or exit though any of those 5 cells based on the non-conservative spin-flip dynamics described above.

4.2 One-Lane Simulation

Using the corresponding one-lane calibrated parameters for J_0 and τ_0 from Sect. 4.1 we now obtain the fundamental diagram (flow—density relationship) in Fig. 6. We refer to Appendix 2 for details on how to construct the fundamental diagram from data and more generally how to collect and report data from observations and simulations. Each data point in this

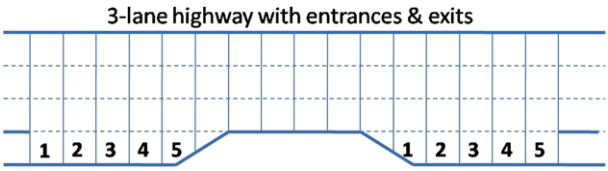

Fig. 5 A depiction of a typical entrance and exit ramp for the highway. We let, for our simulations, these ramps to occupy 5 cells or approximately 110 feet. Vehicles may use any of those 5 cells in order to enter or exit the highway

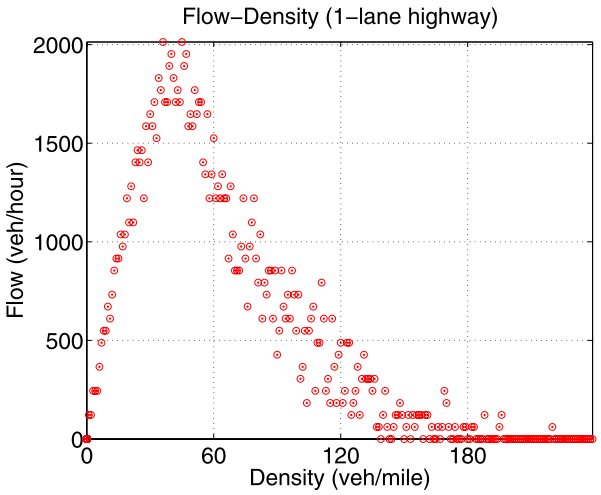

Fig. 6 The flow versus density (fundamental diagram) relationship for 1-lane highway. Spatial periodic length of 1 mile. The presented data has been aggregated over one minute. There is a capacity drop around the critical density region which is in agreement with observations in [31] and [50]. This capacity drop would be even more pronounced if we aggregate data for larger than one minute

figure therefore represents the flow, measured in number of vehicles per hour, sustained for a given density of vehicles, measured in number of vehicles per mile. To create Fig. 6 we use a random initial vehicle distribution and observe the behavior of the traffic stream as density increases incrementally while new vehicles enter the highway. Of course, at times density also decreases as vehicles randomly exit the highway due to our stochastic mechanism.

There is a number of very interesting observations that can be made from Fig. 6. We compare our results with those of Nagel and Schreckenberg [31] for one-lane traffic but also with observations in [50] and observe qualitative agreement. Specifically, the region of free flow is clearly displayed up to approximately 50 vehicles/mile. Although it seems clear from this plot that for densities between 40 and 50 vehicles there can be multiple flows possible. This is a very positive observation since this is typically the case in real traffic. The capacity drop in this figure seems to occur approximately around 50 vehicles. Similarly we observe a maximum vehicle flow of approximately 2000 vehicles/hour which also agrees with observations [32, 50] and Fig. 1(b) from [12].

The fluctuations in vehicle flows shown in Fig. 6 are sizable for densities above c_{crit} and display a widely meta-stable, "stop and go" type, region. We should point out here that we did not fit parameters in order to obtain c_{crit} or q_{max} yet these parameters occurred naturally in our stochastic simulations and are in agreement, for one-lane traffic, with observations of $c_{crit} \approx 50$ vehicles/mile and $q_{max} \approx 2000$ vehicles/hour [50]. This is therefore a further basic validation of our method.

We also should point out that the stop and go traffic effects as well as other non-linear wave phenomena could be understood as resulting from the non-locality of the flux function for a given range of densities. Specifically, we have shown in [44] that the corresponding mesoscopic PDE for the one-lane stochastic model looses its convex form for some values of J_0 (corresponding to those used here). In particular, as can also be seen in Fig. 10 of [44], the flux function stops being convex for the range of densities where stop and go waves have been observed in actual traffic data. Overall therefore we have seen that, at least in the one-lane case, the non-locality of the flux function together with appropriate values of J_0 (or L) can produce non-linear behavior for a range of densities which agree with those observed in real traffic.

4.3 Multi-Lane Simulations and Spatio-Temporal Characteristics

Using the parameters for τ_0 and J_0 from the calibrated simulations presented in Table 1 we now numerically simulate multi-lane highways. In the case of a two-lane highway we present the fundamental diagram (the density—flow relationship) in Fig. 7. There is a number of very interesting observations which can be made from this diagram as well. Note that once again we do obtain realistic values for c_{crit} and q_{crit} which are in agreement with equivalent 2-lane highway data (i.e. $c_{crit} \approx 200/960 = 0.2$ and $q_{crit} \approx 2800$ veh/hour as in [32] and [50]). We also note the lane separation phenomenon which is evident in our simulations as seen in the left plot of Fig. 7. This phenomenon is also commonly observed in actual traffic data. The scatter in the traffic data is evident in both the flow-density and flow-velocity plots of that figure.

The data presented thus far has mainly been of aggregate nature. We will now explore spatio-temporal type information in our simulations. In that respect we simulate a three-lane two-mile section of a highway in Fig. 8 where we observe random formation of jams as well as rarefactions. Below we examine what happens in the case that density abruptly increases past c_{crit} due to an accident blocking one lane on a two-lane highway.

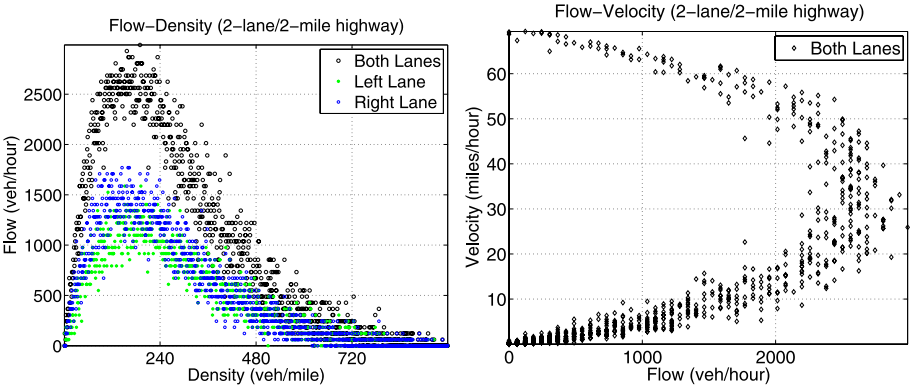

Fig. 7 Flow versus concentration (fundamental diagram) and velocity versus flow relationship for a 2-lane highway. Spatial periodic length of 2 miles, relaxation time $\tau_0 = 2$, interaction strength of $J_0 = 0.6$ while the look-ahead is maintained at $L = 4$. The form of these figures compares favorably with observations in [32, 50] and Figs. 2.10 and 2.14 in [6]

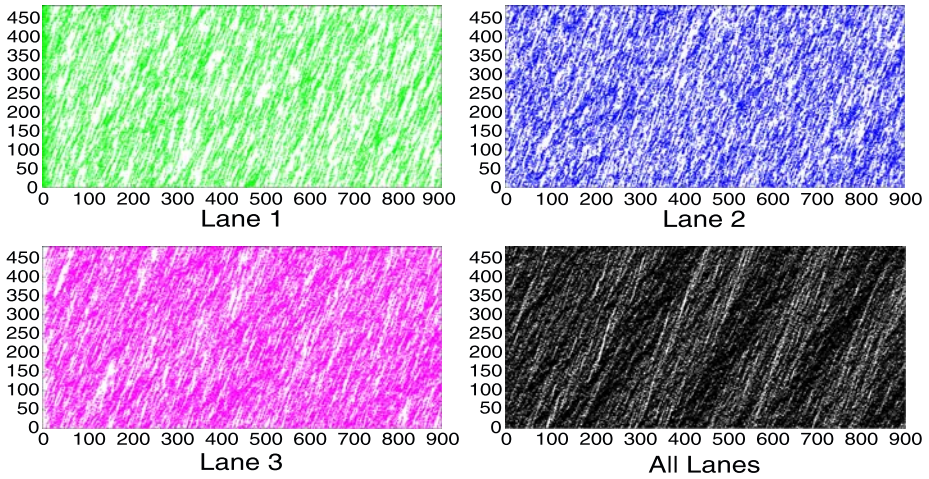

Fig. 8 Traffic development for each lane as well as overall. This is a three-lane highway with entrances and exits. Axis show time (in seconds) vs space (in cells). Phenomena such as retarded acceleration and timely breaking [40]: vehicles slowly speed up when coming out of a jam and similarly start breaking before having reached the jam ahead of them. These phenomena are manifested in the figures above though jam or rarefaction waves. Total time: 15 minutes = 900 seconds

4.3.1 Test Case. Effects of Accident on Flow

In order to further illustrate the type of spatio-temporal information which this model could possibly be used for we record observables under a simulated accident. For this example we model a two mile, two-lane section of a highway. Each lane of the highway therefore consists of 480 cells each of size 22 feet. We allow a total density of 400 vehicles which initially are assumed stopped by a red light. After the light turns green traffic is allowed to commence. We simulate a vehicle collision 15 minutes after the light turned green. The location of this accident is at cell 200 on the highway. The result of the collision is assumed to be that two cells on the inner lane of the 2-lane highway will remain occupied for approximately 20 minutes until the vehicles are cleared. The overall simulation is presented with two plots in Fig. 9. The first plot displays the spatio-temporal information of every vehicle in this 2-lane highway during the whole hour. The second plot presents the flow as it develops over time with data collected from a simulated detector placed at cell 150. Thus the detector is located at a distance of $50 \times 22 = 1100$ feet upstream of the accident. This explains the small delay in detecting the jam downstream in the second plot of Fig. 9. Note the stop and go waves evident after the incident has cleared in the flow-density diagram in Fig. 9. These type of stop and go waves are typical of such high density problems. These waves are clearly marked and in fact we can even measure not only their amplitude but also their period. Also note, once again, the separation between the two lanes evident in the flow diagram in the second plot in that figure.

Overall it seems that there are two types of wave scales in effect here. First there is a large period within which traffic waves propagate and that period can even be measured in our simulations to have a frequency of approximately 5 minutes. Within these 5 minutes however there are other types of wave fluctuations with a smaller time scale and their own period. Further it is also evident from these results that the left (faster) lane has a slightly different period than the right (slower) lane. Note that the left and right lane period mainly

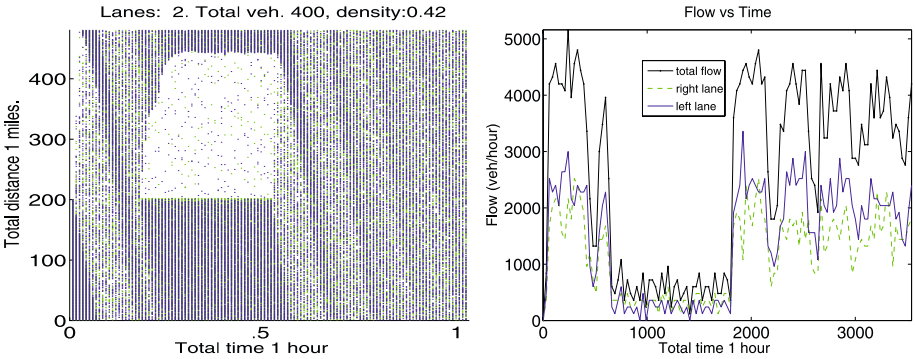

Fig. 9 The detector has been placed upstream of the accident at cell 150, or $50 \times 22 = 1100$ feet from the accident, in this simulation. The duration of this accident is approximately 20 minutes after which the road is cleared. Note the stop and go traffic waves visible after the accident clears

agree at the large scale but seem to disagree in the smaller time scale and in fact seem to contrast each other (i.e at the moment that the flow in the right lane decreases the flow in the left lane increases). Overall however their periods are in agreement for larger time intervals. Note also how the amplitude of these waves seems to be slowly fading away. This effect may be more visible in the left diagram of Fig. 9. The dynamic situation depicted by this simulation, therefore, hints the existence of a metastable state due to the fact that locally there are no entrances or exits, upstream or downstream, which would further increase vehicle concentrations and lead the system to a complete break-down.

5 Comparisons with Other Well-Known Models

There are some similarities and many differences between the model introduced here and those proposed in a, large, number of Cellular Automaton approaches. Specifically CA models are similar to our model mainly in the fact that space is descritized due to the application of a lattice. For our model however velocity as well as time are not discrete but continuous variables. This is in contrast to a large number of CA models or even optimal velocity models [17].

A number of recent, more advanced, CA models involve noise terms in an effort to make predictions less deterministic and eventually more realistic. Using such random terms CA models have been able to reproduce chaotic effects observed in actual traffic data. This however is the extend of the similarities between some of the best CA models and our approach.

A number of differences set apart our stochastic model from even the best CA type models. The most important difference is that our approach is systematic and assures no bias is involved in the dynamics describing the process. More specifically, our stochastic process $\{\sigma_t\}_{t\geq 0}$ relies on the underlying Markov chain which is *memoryless* and *aperiodic* [43]. These properties are critical not only for designing the Markov chain but also in terms of making sure that all possible states of our system have a probability assigned to them through which they could *all* have a chance to be visited (however small that might be). CA approaches on the other hand suffer from the fact that, due to the ad-hoc ways that randomness is included in the model, bias or limit cycles are, unknowingly to the researchers, being introduced in the system. Simply put CA approaches do not really create a stochastic

process but just a deterministic model with some random noise terms and perhaps, even, bias. In that respect therefore our approach is not only different but also safer while trying to extract unknown behavior for a dynamical system.

A significant added benefit for the model presented here is that we can use it in order to produce, based on rigorous mathematics, a closed equivalent PDE for traffic flow. As a result it is possible, at the microscopic level, to observe small time/space effects due to local fluctuations in traffic parameters of interest, while, at longer scales, we can study aggregate behavior and make use of the equivalent macroscopic model to observe long term effects and characteristics of the traffic stream. This type of direct correspondence and derivation from microscopic dynamics to macroscopic PDEs has not been shown (to the knowledge of the authors) for any CA model. In that respect we refer to [44] where this has been carried out and a hierarchy of traffic flow models have been produced, corresponding to different expansions, all of which initiate from a microscopic single-lane traffic model.

5.1 Mesoscopic Derivations

A number of PDE type traffic flow models exist treating the multi-lane highway case. Most such models start from a macroscopic description such as the Boltzmann, gas-kinetic, equation [10], compressible fluid [41] or similar equation [14] and undertake a detailed description of vehicle interactions per lane. These terms are then included on the right hand side of those equations in order to model vehicle interactions among lanes. Other approaches use hybrid systems of PDEs coupled to order parameter models [24], optimal velocity models [29] and even time dependent Ginzburg-Landau descriptions [28].

We provide below, without proof or details, the mesoscopic PDEs corresponding to the multi-lane local mean field approximation of the microscopic stochastic model developed here. The full details of this derivation will be included in a future publication. The case of a single lane highway was treated in [44]. Based on the law of large numbers and appropriate asymptotic expansions we obtain the following traffic multi-lane PDEs,

$$\begin{aligned} &u^i_t + c_0[u^i(1-u^i)\exp(C(u))]_z \\ &\quad = c_0[J_1 u^i(1-u^i)\exp(C(u))u^i_z]_z + c_0[J_2 u^i(1-u^i)\exp(C(u))u^i{}_{zz}]_z \end{aligned} \tag{17}$$

where the index $i = 1, 2, 3\ldots$ signifies the lane number, $u^i = E\sigma_i$ represents the average density per lane and J_0, J_1, J_2 from the Taylor expansion of the interparticle potential $J(x, y)$ in (3). Note that the coupling occurs in the exponential function $\exp(C(u))$, whose details will be included in a future publication, includes contributions from all lanes. That function is only a linearization of the corresponding convolution term contributed from the interaction potential function U in (8).

Furthermore we note that (17) is a third order dispersive-diffusive PDE similar in form to the PDEs derived from optimal velocity models (usually referred to as "modified" KdV). Equation (17) is hierarchical in the sense that if we let $J(x, y) \equiv 0$ we obtain a

$$\text{Lighthill-Whitham-Richards (LWR) type equation:} \quad u^i_t + c[u^i(1-u^i)]_z = 0. \tag{18}$$

If instead $J_1 = J_2 = 0$ we obtain an advective-diffusive

$$\text{Burger's type contribution:} \quad u^i_t + c[u^i(1-u^i)\exp(-J_0 u)]_z = 0 \tag{19}$$

which has a non-convex flux. Several more models and connections to classical traffic PDEs can be obtained by analyzing (17) further [44].

We should point out similarities between the proposed multi-lane PDEs in (17) and those found in the literature. It is interesting to note that several models for multi-lane traffic follow a similar form as that derived in (17). In particular, Illner, Klar and Materne provide a system of hyperbolic type integrodifferential PDEs in (2.1) of [14], one for each lane, starting from a Vlasov-Fokker-Planck type description under suitable assumptions. The right hand side of those mainly hyperbolic type PDEs consist of integrodifferential terms involving interactions due to braking and acceleration of vehicles per lane. Similarly Helbing [10] produced a multi-lane traffic flow PDE starting from a Boltzmann type description. A system of two coupled equations per lane is produced in (63) and (64) of [10]. The first equation describes density per lane while the second describes velocity per lane. The overall system although quite involved is hyperbolic in nature with nonlinear diffusion and reaction terms on the right hand side for each lane. A similar such derivation can be found in [21] where once again equations (4.6) and (4.7) describe a hyperbolic PDE for each lane although its right hand side include contributions from sinks and sources due to lane changing. Furthermore equation (4.6) in [21] is coupled to another hyperbolic type PDE per lane (4.7) with more interactions in its right hand side. The overall system could once again be described a hyperbolic nonlinear diffusion reaction PDE per lane with several nonlinear interaction terms on the right hand side. Finally, in another work in [24] the authors provide a multi-lane traffic PDE for vehicle density similar in form to (19) above which is coupled to a hyperbolic type PDE for an order parameter h whose values varies from 0 to 1 and describes multilane correlations in vehicle flow.

6 Conclusions and Future Directions

In this work we developed a multi-lane stochastic traffic flow model which relies on a mixture of microscopic conservative and non-conservative Arrhenius dynamics in order to realistically reproduce the behavior of actual traffic. The model relies on two main traffic parameters J_0 and τ_0. These parameters are easily calibrated since they are directly linked to known values from traffic observations. A third independent variable is the look-ahead range L which is related to the perceived physical length within which drivers interact with their surrounding environment. Last the lane changing constant k depends on traffic rules enforced in different countries. Using these parameters we were able to provide solutions of our model via kinetic Monte Carlo simulations which compare favorably with actual traffic data.

The multi-lane stochastic model presented here has been shown to have several important properties and advantages such as: (a) ease in calibration, (b) no *ad-hoc* noise is introduced, (c) captures correctly quantities of interest such as maximum flow q_{crit} and critical density c_{crit}, (d) timely breaking, (e) retarded acceleration, (g) lane separation.

A very interesting phenomenon was discovered during the hypothetical traffic accident simulation which leads us to believe that the stochastic processes responsible for vehicle interactions operate at different scales. This multi-time scale phenomenon which is revealed when analyzing flows between different lanes for concentrations above c_{crit} could be responsible for many of the well-known stop and go (meta-stability) waves which have been known to occur for such densities or after accidents. This is an intriguing question which warrants further research. In that respect the periods hidden within the larger scales for each lane should also be statistically examined and their cross/correlations revealed.

A number of possible approaches are suggested below which can lead to significant improvements for this stochastic traffic model.

(a) As an alternative we can calculate the interaction potential (8) through a bell-shaped (Gaussian) curve instead of the currently used uniform rule (5). In that respect the strength of the local interactions between vehicles will increase as their distance becomes smaller.
(b) Another possible modification which can make this model even more realistic in terms of driver behavior is to allow the look-ahead parameter, L, to be a variable instead of a constant. It would be more realistic to have L vary with respect to the density of vehicles on the road. For example, if there is a low density of vehicles, then drivers can conceivably see further ahead than in a high density section of highway where vehicles are bumper-to-bumper.
(c) Another consideration is how our model could handle non-homogeneous traffic. This distinction of different types of vehicles could potentially allow us to reproduce the empirical data in [50] (which includes 10% trucks) even more realistically. There are two possible methods to incorporate this into our dynamics: we could count each truck as multiple passenger cars as is often done, or we could model the effect of trucks by giving 10% of vehicles a lower maximum velocity as is done in [32]. Our model could be easily adapted for the latter approach through the parameter τ_0.

Acknowledgements The research of T.A. and A.S. is partially supported by NSF DMS 0606807 and NSF DMS 0836699. This work was supported, in part, by funds provided by the University of North Carolina at Charlotte. The authors would also like to acknowledge valuable comments and recommendations by the Referees which helped to further the content and novelty of this work.

Appendix 1: Monte Carlo Pseudo-Code

Overall the spin-flip and spin-exchange algorithm with Arrhenius dynamics, has the form:

Spin-Flip and Spin-Exchange Kinetic Monte Carlo Pseudo-code

1. Calculate all transition rates $c^a(l)$ (absorption), $c^d(l)$ (desorption), from (12) and $c^e(l)$ (exchange), from (6) for *all* nodes l in the lattice.
2. Calculate the total $R_a = \sum_l c^a(l)$, $R_d = \sum_l c^d(l)$ and $R_e = \sum_l c^e(l)$ absorption, desorption and exchange rates respectively. Obtain the total rate $R = R_a + R_d + R_e$ based on above.
3. Obtain a random number, say ρ.
4. Index all rates in an array c of size $3|\mathcal{L}|$.
5. Find the node at lattice position k where $0 < k < 3|\mathcal{L}| - 1$ such that,

$$\sum_{j=0}^{k} c(j) \geq \rho R > \sum_{j=0}^{k-1} c(j). \tag{20}$$

6. Update the time, $t = t + \Delta t$ where $\Delta t = -1/\log(c(k)/R)$.
7. Repeat from step 1 until dynamics of interest have been captured.

This pseudo-code gives only a rough outline of the main algorithm. There are several techniques, not listed here, which allow for significant speed-up for each of the main steps presented above.

Appendix 2: Data Collection: Virtual Versus Actual Detectors

The Monte Carlo simulations which we undertake here allow the placement of virtual detectors at specified locations in an effort to reproduce real traffic data collection procedures. As a result the virtual data collected from our simulations can be easily compared to actual data collected with an equivalent method from a real highway.

Pneumatic loop detector facilitate some of the most common data collection methods in traffic. These detectors are small hollow tubes attached to an electronic counting device. These detectors are placed on the highways in order to record the location and speed of each passing vehicle as well as local traffic density.

The ways of collecting and recording actual traffic information can be found in [2, 6, 26, 34]. The flow, q, is measured as the number of vehicles $n(\tau)$ passing a detector at a given time interval τ via,

$$q = \frac{1}{\tau} n(\tau). \tag{21}$$

Based on this formulation flow cannot be found from a single snapshot of vehicles over an interval. Another point of contention among research is that flow is usually measured in units of number of vehicles *per hour* although the actual time length of recorded observation is much shorter (only a few minutes). This type of data manipulation leads to questions of sustainability of such high volumes when in fact measurements were performed over time intervals which are less than 15 minutes long [7].

Density, c, on the other hand, is quite difficult to ascertain using empirical measurements [26]. At best density is measured along a length [6]. If this is not practically possible however it is common for practitioners to measure density through the well-known macroscopic formula

$$q = c\bar{v} \tag{22}$$

which states that flow is the product of mean speed and density [48]. (Mean speed here implies space mean speed as opposed to time mean speed. See [44] for some details.)

In the results shown in this work, we compute flow from (21) while density is found through calculation of occupancy in the same fashion as done in [31], by averaging the data over small intervals of time. This method of measuring occupancy is very similar to actual traffic data collection practices. We provide all the details of the parameters used in each of the simulations in Sect. 4.

In the cases of simulations with highways which include entrances and exits we place the virtual detector at a small distance downstream of their location. This allows to detect density changes in the highway shortly after they occur.

Finally we note that in this work we simulate a circular highway with entrances and exits which is 1 mile long. Any length of highway can be accommodated however. Vehicles are initially randomly distributed on the highway. On the other hand, construction of fundamental diagrams (density-flow relationship) requires extensive simulations so that densities at most ranges will be encountered. In this case we initialize the simulation with very few vehicles and allow an abundance of vehicles to enter so as to collect information as density gradually increases. When presenting the fundamental diagrams we only use data for which the local density has been sustained for at least 30 seconds.

References

1. Akcelic: Traffic models-research and software for the transport industry (2007). http://www.sidrasolutions.com, accessed Oct. 10
2. Athol, P.: Interdependence of certain operational characteristics within a moving traffic stream. In: Highway Research Record, pp. 58–97 (1972)
3. Aw, A., Rascle, M.: Resurrection of "second order" models of traffic flow. SIAM J. Appl. Math. **60**, 916 (2000)
4. Bortz, A.B., Kalos, M.H., Lebowitz, J.L.: A new algorithm for Monte Carlo simulations of Ising spin systems. J. Comput. Phys. **17**, 10 (1975)
5. Daganzo, C.F.: Requiem for second-order fluid approximations of traffic flow. Transp. Res. B **29**, 277 (1995)
6. Hall, F.L.: Traffic Flow Theory, pp. 2–34. US Federal Highway Administration, Washington (1996)
7. HCM: Highway capacity manual. Tech. rep., Transportation Research Board (1985)
8. HCM: Highway capacity manual. Tech. rep., Transportation Research Board, Washington, DC (2000)
9. Helbing, D.: Gas-kinetic derivation of Navier-Stokes-like traffic equations. Phys. Rev. E **53**(3), 2366 (1995)
10. Helbing, D.: Modeling multi-lane traffic flow with queuing effects. cond-mat.stat-mech (1998)
11. Helbing, D.: Traffic and related self-driven many-particle systems. Rev. Mod. Phys. **73**(4), 1067 (2001). cond-mat/0012229
12. Helbing, D., Hennecke, A., Shvetsov, V., Treiber, M.: Micro and macro simulation of freeway traffic. Math. Comput. Model. **35**, 517 (2002)
13. Hildebrand, M., Mikhailov, A.S.: J. Phys. Chem. **100**, 19089 (1996)
14. Illner, R., Klar, A., Materne, T.: Vlasov-Fokker-Planck models for multilane traffic flow. Commun. Math. Sci. **1**, 1 (2003)
15. Jiang, R., Wu, Q.S.: Cellular automata models for synchronized traffic flow. J. Phys. A **36**(2), 281 (2003)
16. Jin, S., Liu, J.G.: Relaxation and diffusion enhanced dispersive waves. Proc. R. Soc. Lond. A **446**, 555–563 (1994)
17. Kanai, M., Nishinari, K., Tokihiro, T.: Stochastic optimal velocity model and its long-lived metastability. Phys. Rev. E **72** (2005)
18. Katsoulakis, M., Sopasakis, A., Plechac, P.: Error analysis of coarse-graining for stochastic lattice dynamics. SIAM J. Numer. Anal. (2006)
19. Kerner, B.S., Klenov, S.L.: A microscopic model for phase transitions in traffic flow. J. Phys. A **35**, 31 (2002)
20. Kerner, B.S., Klenov, S.L., Wolf, D.E.: Cellular automata approach to three-phase traffic theory. J. Phys. A: Math. Gen. **35**, 9971 (2002)
21. Klar, A., Wegener, R.: A hierarchy of models for multilane vehicular traffic i: modeling. SIAM J. Appl. Math. **59**(3), 983–1001 (1995)
22. Kurtze, D.A., Hong, D.S.: Traffic jams, granular flow, and soliton selection. Phys. Rev. E **52**, 218–221 (1995)
23. Liggett, T.M.: Interacting Particle Systems. Springer, Berlin (1985)
24. Lubashevsky, I.A., Mahnke, R.: Order parameter model for unstable multilane traffic flow. cond-math/9910268 v2 (2000)
25. Masi, A.D., Orlandi, E., Pressuti, E., Triolo, L.: Proc. R. Soc. Edinb. A **124**, 1013 (1994)
26. McShane, W.R., Roess, R.P.: Traffic Engineering. Prentice-Hall, Englewood Cliff (1990)
27. Muramatsu, M., Nagatani, T.: Phys. Rev. E **60**, 180 (1999)
28. Nagatani, T.: Jamming transitions and the modified Korteweg-de Vries equation in a two-lane traffic flow. Physica A **265**, 297–310 (1999)
29. Nagatani, T.: Stabilization and enhancement of traffic flow by the next-nearest-neighbor interaction. Phys. Rev. E **60**, 1535 (1999)
30. Nagatani, T.: The physics of traffic jams. Rep. Prog. Phys. **65**, 1331 (2002)
31. Nagel, K., Schreckenberg, M.: A cellular automaton model for freeway traffic. J. Phys. I **2**, 2221 (1992)
32. Nagel, K., Wolf, D.E., Wagner, P., Simon, P.: Two-lane traffic rules for cellular automata: a systematic approach. Phys. Rev. E **58**(2), 1425 (1998)
33. Nelson, P.: Phys. Rev. E **61**, 383 (2000)
34. Nelson, P.: On two-regime flow, fundamental diagrams and kinematic-wave theory. In progress (2004)
35. Newell, G.F.: Nonlinear effects in theory of car following. Oper. Res. **9**, 209–229 (1961)
36. Newell, G.F.: Transp. Res. B **23**, 386 (1989)
37. Phillips, W.F.: Transp. Plann. Technol. **5**, 131 (1979)
38. Rathi, A.K., Lieberman, E.B., Yedlin, M.: Transp. Res. Rec. **61**, 1112 (1987)
39. Ross, P.: Transp. Res. B **22**, 421 (1988)

40. Schadschneider, A.: Traffic flow: a statistical physics point of view. Physica A **312**, 153 (2002)
41. Schreckenberg, M., Wolf, D.E.: Traffic and Granular Flow. Springer, Singapore (1998)
42. Sopasakis, A.: Unstable flow theory and modeling. Math. Comput. Model. **35**(5–6), 623 (2002)
43. Sopasakis, A.: Stochastic noise approach to traffic flow modeling. Physica A **342**(3-4), 741–754 (2004)
44. Sopasakis, A., Katsoulakis, M.A.: Stochastic modeling and simulation of traffic flow: ASEP with Arrhenius look-ahead dynamics. SIAM J. Appl. Math. **66**(3), 921–944 (2006)
45. Sparmann, U.: Spurwechselvorgänge auf zweispurigen Bab-Richtungsfahrbahnen. In: Forschung Straßenbau und Straßenverkehrstechnik. Bundesminister für Verkehr, Bonn-Bad Godesberg (1978)
46. Spohn, H.: Large scale dynamics of interacting particles. Springer, Berlin (1991)
47. Vlachos, D.G., Katsoulakis, M.A.: Derivation and validation of mesoscopic theories for diffusion of interacting molecules. Phys. Rev. Lett. **85**(18), 3898 (2000)
48. Wardrop, J.G.: Some theoretical aspects of road traffic research. Proc. Inst. Civ. Eng. Part II **I**, 325 (1952)
49. Whitham, G.B.: Linear and Nonlinear Waves. Wiley, New York (1974)
50. Wiedemann, R.: Simulation des Straßenverkehrsflusses. Schriftenreihe des Instituts für verkenhrswesen der Universität Karlsruhe, vol. 8, Germany (1974)
51. Wright, P.H., Dixon, K.: Highway Engineering, 7th edn. New Jersey (2004)